Scientific Research Report

Combining 3D Multi-Object Reconstruction with Finite Element Analysis for Accurate Dental Modelling and Restoration

Rawan N. AlKahtani [a*], *Yazan M. Allawi* [b*], *Ghadah M. Aladhyani* [a], *Raghad A. Altassan* [a], *Sara S. AlShalawi* [a], *Tamer M. Nassef* [c]

[a] *Department of Clinical Dental Sciences, College of Dentistry, Princess Nourah bint Abdulrahman University, Riyadh, Saudi Arabia*

[b] *Department of Electrical Engineering, College of Engineering, Princess Nourah bint Abdulrahman University, Riyadh, Saudi Arabia*

[c] *Faculty of Computer Sciences, October University of Modern Sciences and Arts (MSA), 6th of October City, Egypt*

ARTICLE INFO

Article history:
Received 9 July 2025
Received in revised form
2 November 2025
Accepted 17 November 2025
Available online 24 December 2025

Key words:
3D multi-object reconstruction
Finite element analysis
Finite element modelling
Dental models
Digital modelling
Biomechanical behaviour

ABSTRACT

Introduction and aims: This study present a novel approach to dental digital modelling that combines 3D multi-object reconstruction with Finite Element Modelling (FEM) to create anatomically accurate and biomechanically stable dental models. The proposed approach overcomes limitations of traditional imaging techniques, such as resolution constraints, artifacts, noise, and poor soft tissue contrast, enabling precise analysis of stress distribution and material behaviour.

Methods: A 3D model of a right maxillary central incisor (tooth no. 11) was developed and adapted into 4 variations receiving various prosthetic treatments: fibre post, resin core, and lithium disilicate crown (Model A); fibre post, resin core, and monolithic zirconia crown (Model B); lithium disilicate endocrown (Model C); and monolithic zirconia endocrown (Model D). Models and prosthetic treatments were created in accordance to dimensions reported in the literature.

Results: Preliminary Finite Element Analyses (FEAs) were performed to evaluate the mechanical behaviour and structural integrity of the models. Under a static load of 100 N applied at a 45° angle, the simulations revealed no significant deformations or irregular stress concentrations. Model A consisted of 33,235 nodes and 19,718 elements, while the simpler design of Model C reduced computational demands to 28,660 nodes and 17,253 elements. Monolithic zirconia, with an elastic modulus of 202,767 MPa, demonstrated superior structural stability across all simulations.

Conclusion: By integrating evidence-based material and structural properties, our approach consistently produces semi-realistic models with adequate mesh density, enabling accurate representation of oral dynamics and precise force transmission across model components.

Clinical Relevance: These findings suggest that anatomically accurate dental models generated through advanced digital modelling and analysed using FEA can realistically simulate occlusal forces, offering a reliable platform for assessing new therapeutic dental approaches and improve upon existing treatment methods to optimise clinical outcomes and patient satisfaction.

* *Corresponding authors*. Department of Clinical Dental Sciences, College of Dentistry, Princess Nourah bint Abdulrahman University, P. O. Box 84428, Riyadh, Zip Code 11671, Saudi Arabia; Department of Electrical Engineering, College of Engineering, Princess Nourah bint Abdulrahman University, P.O. Box 84428, Riyadh, Zip Code 11671, Saudi Arabia.

E-mail addresses: rnalkahtani@pnu.edu.sa (R.N. AlKahtani), ymallawi@pnu.edu.sa (Y.M. Allawi).

Rawan N. AlKahtani: http://orcid.org/0009-0006-8251-1489
Yazan M. Allawi: http://orcid.org/0000-0002-9635-5951
Tamer M. Nassef: http://orcid.org/0000-0001-5301-6848

https://doi.org/10.1016/j.identj.2025.109318

Introduction

Over the past 2 decades, digital modelling has emerged as an important tool in the medical field, especially within dentistry, where it plays an essential role in initial diagnosis, treatment planning, and periodic patient follow-up.[1-3] Recent advancements, driven by artificial intelligence (AI), have further enhanced digital modelling by enabling the creation of highly realistic virtual environments that closely mimic real-world conditions.[4,5] These innovations have significantly enhanced the precision, reliability, and clinical applicability of research findings.[6] Three dimensional (3D) reconstruction is one of the digital modelling methods widely adopted by dental researchers to create semirealistic models. These models can be used to test treatment scenarios, assess their potential effectiveness before applying them to patients, and improve traditional treatment methods. Many studies utilise medical imaging, such as Computed Tomography (CT) and Cone Beam Computed Tomography (CBCT), for providing data input and for the accurate construction of models.[7,8] A significant limitation of this method, however, is its reliance on high quality imaging data as an essential requirement for the accurate construction of dental models.[9] An alternative methodology is the multi-part method, also known as the multi-object reconstruction modeling.[10] This approach involves dividing the structure to be built into multiple objects based on material properties and terrain composition. Each part is reconstructed separately before reassembling all the objects into a complete model. The advantages of this method include facilitating the reconstruction process, reducing the complexity of training, and allowing for precise control of the load on each object.[11,12]

When combined with Finite Element Analysis (FEA), multi-object reconstruction modelling has been instrumental in improving the accuracy and control in biomechanical studies. FEA has emerged as a transformative tool in dentistry, providing unparalleled insights into the biomechanical behaviour of teeth, implants, and surrounding tissues. For example, FEA has been utilised to assess the stress distribution in dental implants subjected to different loading conditions, which guides the design and placement of implants to improve durability and patient outcomes.[13] This computational technique enables dentists to simulate the mechanical forces acting on the dentition, allowing them to optimise treatment approaches. Moreover, FEA helps dentists predict the risk of fractures, debonding of restorations, or other possible complications, where this information are utilised in guiding the selection of appropriate restorative materials and in designing restorations that can withstand the functional demands of the oral cavity, thereby ensuring their longevity and reducing the risk of future failures.[6]

Finite Element Modelling (FEM), a core component in FEA, is widely used to address complex geometric challenges, especially when analytical solutions to complex mechanical problems are difficult to achieve. FEM works by dividing the problem domain into smaller, simpler elements, allowing for the analysis of stress distribution and deformation patterns, making it crucial in biomechanical studies.[13] For instance, FEM has been employed in[14] to optimise attachment designs in implant-supported removable prostheses, demonstrating that flexible Nitinol-based components significantly reduce strain and wear at the male-female interface, improving prosthesis longevity and patient comfort. The work in[15] conducted a finite element comparison of 3-piece, 2-piece, and 1-piece dental implant systems in the molar region revealed that 2-piece ceramic implants demonstrated superior stress distribution and strain reduction, showing their biomechanical advantages for improved implant stability and longevity. Additionally, a finite element analysis of Ti-base abutment heights in implant-supported prostheses in[16] revealed that increased abutment height leads to higher stress transfer and deformation within physiological limits, emphasizing the need for optimised abutment selection to balance biomechanical and biological factors.

This study introduces a methodological framework to digital modelling by constructing a semirealistic model of a right maxillary central incisor (tooth no. 11) receiving various prosthetic treatments. These models are nonpatient specific, reproducible, with literature-based dimensions and material properties instead of digital image sources. By integrating 3D multi-object reconstruction with FEA techniques, this study aims to accurately construct models and restorations, enabling precise and controlled analysis of stress distribution and material behaviour, while eliminating anatomic variability between patients. This approach highlights the potential of constructing shareable dental digital models with high precision using advanced, computationally efficient, digital modelling techniques combined with evidence-based data to realistically simulate real-life conditions and provide reliable and accurate results.

Materials and methods

Models and prosthetic design

A 3D model of a right maxillary central incisor (tooth no. 11) was constructed in accordance to dimensions reported in the literature, as summarised in Tables 1 and 2, to ensure anatomical accuracy. The model was duplicated to form the four distinct variations illustrated in Figure 1, such that:

1. Model A: Root canal treated using gutta-percha and an endodontic resin sealer and coronally sealed using a fibre post constituting of quartz/ glass fibres in an epoxy resin matrix, a composite resin core, and a lithium disilicate crown.
2. Model B: Root canal treated using gutta-percha and an endodontic resin sealer and coronally sealed using a fibre post constituting of quartz/ glass fibres in an epoxy resin matrix, a composite resin core, and a monolithic zirconia crown.
3. Model C: Root canal treated using gutta-percha and an endodontic resin sealer and coronally sealed using a lithium disilicate endo-crown extending down the coronal 5 mm of the root canal.
4. Model D: Root canal treated using gutta-percha and an endodontic resin sealer and coronally sealed using a monolithic zirconia endo-crown extending down the coronal 5 mm of the root canal.

Table 1 – Evidence-based dimensions and properties of dental and periodontal structures.

Constitutes	Properties	Values	References
Tooth dimension	Length	1. Total length: 22.5 mm 2. Length of crown: 10.5 mm 3. Medial-distal width: 8.5 mm 4. Root length: 12 mm	17
Enamel	Elastic modulus	8.41×10^4 MPa	18
	Poisson's ratio	0.30	
Root dentin	Thickness	1. Buccal: 2.68 mm 2. Lingual: 2.72 mm 3. Mesial: 1.82 mm 4. Distal: 1.85 mm	19
	Elastic modulus	18,400 MPa	20,21
	Poisson's ratio	0.31	
Cementum	Thickness	1. Coronal 2/3: 36.5 microns 2. Apical 1/3: 169.55 microns	22,23
	Elastic modulus	15,000 MPa	20,21
	Poisson's ratio	0.31	
Periodontal ligament	Thickness	0.22 mm	24,25
	Elastic modulus	68.9 MPa	26,27
	Poisson's ratio	0.45	
Alveolar bone	Thickness	1. Buccal: 1 mm 2. Alveolar crest: 0.82 mm 3. Palatal: 3 mm apical to Alveolar crest: ≈ 2 mm 4. Mesial: 3 mm 5. Distal: 3 mm	28-34
	Elastic modulus	137,000 MPa	20,35
	Poisson's ratio	0.30	

The dimensions, mechanical properties, and material characteristics in each model were derived from evidence-based data and are detailed in Tables 1 and 2, respectively. In models A and B, receiving the contemporary prosthetic treatment, the fibre post length was 11 mm (5 mm in the crown and 6 mm in the root), ensuring the post length exceeded the clinical crown length of 10.5 mm.[56] The dimensions of the fibre post adhered to the size 2 RelyX fibre post, commonly used for maxillary central incisors.[57] Assuming the sulcus depth is 1.5 mm[58] and considering the CEJ is in relation to the junctional epithelium, the finish line was set 1 mm above the CEJ, followed by a 2 mm ferrule effect. The alveolar bone crest was positioned 2 mm apical to the CEJ and 3 mm apical to the finish line to preserve the biological width.[59] This complex, multi-layered 3D multi-object reconstruction model allowed for a 2-wall ferrule effect. Therefore, a 2 mm labial and palatal ferrule were created, which are crucial for the fracture resistance and retention of the crown in anterior endodontically treated maxillary teeth.[60-62] To address the limitation of missing ferrules on the mesial and distal aspects, mesial and distal resin plugs or projections were created to simulate a ferrule, which can potentially provide an antirotational feature to the prosthetic design.

3D multi-object reconstruction

The reconstruction of 3D models was carried out using the method proposed in,[63] which employs triangulation theory to initially generate 2.5D surface representations of the right maxillary central incisor (tooth no. 11). These intermediate models were subsequently refined into full 3D volumetric representations using the marching cubes algorithm expressed in Equations (1) and (2), with the results as illustrated in Figures 2 and 3, respectively. All processing and model generation were performed in MATLAB (R2023b).[64] To ensure accuracy, the resulting triangle mesh of the tooth must define a closed 2-manifold to precisely represent a volume and enable 3D meshing. This guarantees that no vertex in the triangle mesh is complex, and each edge of the triangle mesh is shared by exactly 2 triangles, adhering to the dimensions, mechanical properties, prosthetic materials, and design characteristics reported in the dental literature to ensure reproducibility and minimise intersample variability.

$$\frac{x_{data} - x_{pixel}}{f} + \frac{m_{11}(x_j - x_s) + m_{12}(y_j - y_s) + m_{13}(z_j - z_s)}{m_{31}(x_j - x_s) + m_{32}(y_j - y_s) + m_{33}(z_j - z_s)} = 0 \quad (1)$$

$$\frac{y_{data} - y_{pixel}}{f} + \frac{m_{21}(x_j - x_s) + m_{22}(y_j - y_s) + m_{23}(z_j - z_s)}{m_{31}(x_j - x_s) + m_{32}(y_j - y_s) + m_{33}(z_j - z_s)} = 0 \quad (2)$$

In its artistic application, the marching cubes algorithm constructs a set of triangles without considering neighbourhood connectivity or enforcing topological constraints. Consequently, the generated triangle mesh may contain complex vertices and edges shared by more than 2 triangles. These issues typically occur when one or more intersections between the cube's edges and the object align with a vertex P_{ijk} of the cube as depicted in Figure 3. In such cases, the predefined triangle configurations stored in the lookup tables of the marching cubes algorithm may lead to degenerate elements, such as collapsed edges or singular vertices.[65]

Finite element modelling

After multi-object reconstruction, the objects were enveloped by texture material before all planes are assembled to verify their mechanical properties and alignment with design specifications. This was accomplished by evaluating the vertex coordinates (x, y, z) of the model relative to the origin (0, 0, 0),

Table 2 – Evidence-based material and design dimensions and properties.

Constitutes	Properties	Values	References
Gutta percha (GP)	Length	4 mm	36
	Distance between GP and root apex	2 mm	37,38
	Elastic modulus	0.69 MPa	27,39
	Poisson's ratio	0.45	
Resin cement	Thickness	75 μm	40,41
	Elastic modulus	9,267 MPa	42,43
	Poisson's ratio	0.27	
Composite resin core	Elastic modulus	18,000 MPa	44
	Poisson's ratio	0.30	
Fibre post	Dimensions	1. Diameter: 1.6 mm 2. Taper: 0.08 mm 3. Taper length: 10 mm (size 2 RelyX red) 4. Total length: 11 mm (5 mm in crown and 6 mm in root)	45
	Depth of embedded post in resin core	4 mm	46
	Elastic modulus	40,000 MPa	47,48
	Poisson's ratio	0.28	
Endocrown lithium disilicate (LD)/ Monolithic zirconia (MZ) crowns	Core depth into root canal	4 mm	49,50
	Thickness	1. Incisal 2 mm reduction 2. 0.8 mm deep reduction chamfer margin 3. 1-1.5 mm middle third reduction	18
	Elastic modulus (LD)	95,000 MPa	51,52
	Poisson's ratio (LD)	0.30	
	Elastic modulus (MZ)	202,767 MPa	50,53
	Poisson's ratio (MZ)	0.325	
	Ferrule effect	2 mm	54,55

from which pixel positions can be calculated. In FEM, the mechanical intensity is measured according to (3) by calculating the pixel values multiplied by the number of pixels.

$$Intensity(x) = \sum_{i=1}^{N} (P_n * P_v) \quad (3)$$

In this process, P_n represents the pixel position, P_v is the corresponding pixel value, and i indexes the individual pixels. The next phase involved generating 3D solid meshes of the anatomical structures and integrating them into a unified model using ANSYS (Release 14).[66] To facilitate this, surface models of the 3 components were imported in STL (Surface Tessellation Language) format, commonly used for representing bone geometry. Meshing involves the discretization of a continuous object into a finite number of smaller elements.[67] In solid meshing, the interior of a hollow model is populated with volumetric elements, forming a complete solid mesh. For the tooth model, the process began by importing the tooth's surface geometry, which was then validated to detect and correct any cross elements by overlapping mesh elements or inside-out elements with surface normal facing inward.[68] To ensure the surface was watertight and suitable for solid meshing, nodes located within 0.001 cm from each other were merged using the sweep command, which helps creating a continuous, closed surface and eliminate any cross elements. Following this, the Patran Tetrahedral meshing was applied, resulting in a high-quality solid mesh composed of 4-node tetrahedral elements.[69-72]

The generated mesh exhibited skewness values below 0.40, aspect ratios under 5.0, and valid Jacobian determinants across all elements, indicating geometric correctness and numerical stability. Convergence was confirmed when further mesh refinement produced von Mises stress variations on the cortical bone at ≤5%. The element size was reduced by approximately 20%, resulting in a smooth transitional growth rate of 1.2 was implemented and element sizes ranged from 0.002mm to 0.823mm. The meshing specifications are detailed in Tables 3 and 4 and illustrated in Figure 4.

Preliminary FEA were conducted to assess the mesh sensitivity and structural integrity of the computational models under a defined loading condition for experimental verification. A static load of 100 N was applied to a circular area with a 3 mm diameter, cantered on the lingual fossa (refer to Figure 5 for precise location). The model represented a tooth with a 5° proclination relative to a defined reference plane. The applied load vector was then oriented at a 45° angle relative to the long axis of the tooth, approximating the occlusal forces generated during functional contact with an antagonist tooth during mastication.[18,73,74] Constraints were applied at the outer alveolar bone surface fixed in all degree of freedoms (DOFs). The loading was static and time-independent. Materials were modelled as linear-elastic, homogeneous, and isotropic evaluated under standard laboratory conditions (ambient temperature, dry, no aging/swelling). Interfaces for the stability checks were idealised as bonded (tied) between crown-cement-tooth components; no frictional contact or cohesive/failure laws were activated. Analyses were performed in ANSYS Mechanical, Static Structural System, using the sparse direct solver with program-controlled (default) convergence controls; large-deflection effects were disabled and double precision was enabled. Linearity was verified by repeating the analysis at 2× the baseline load and evaluating the normalised ratio with an acceptance of 2.00 ± 0.05.

The overall modelling and verification process was conducted in accordance with the principles of the NAFEMS Engineering Simulation Quality Management Standard (ESQMS, 2020) to ensure traceability, transparency, and reproducibility of the computational workflow.

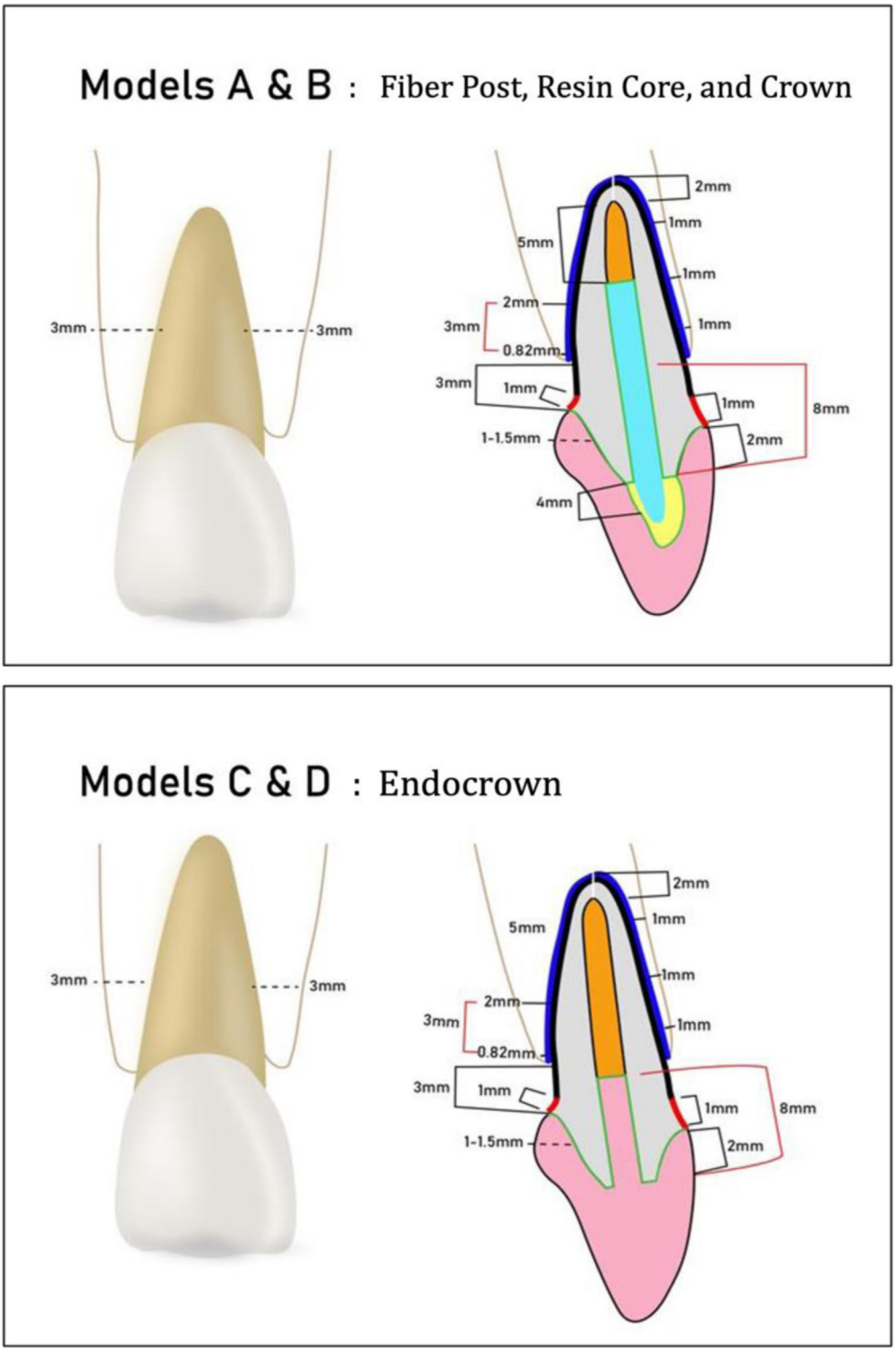

Fig. 1 – Dimensions of the 3D multi-object reconstruction models A and B, and C and D.

Statistical analysis

Finite-element (FE) models are deterministic systems. Once the geometry, materials, boundary conditions, and solver options are fixed, they return the same output on every run. This differs from laboratory testing, where natural scatter and measurement noise introduce random variability. Since a FE result is not a sample drawn from a distribution, summary statistics such as means and standard deviations are not informative for a single, fixed-input simulation.

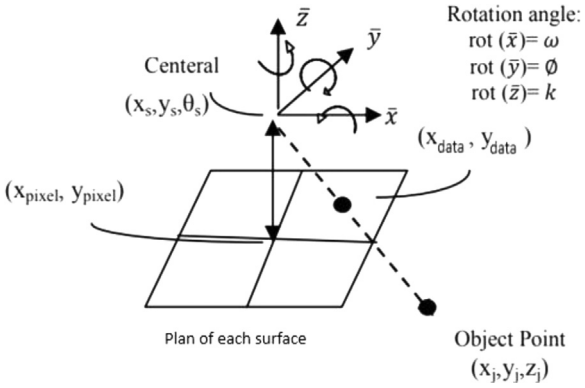

Fig. 2 – Nomenclature for the triangulation equations used to create 3D models.[2]

Results

Exploded mesh models receiving conventional prosthetic designs (A and B) and models receiving endocrowns (C and D) are shown in Figure 6. The meshing process highlighted the importance of maintaining anatomical accuracy while achieving computational efficiency, which was achieved using the 3D multi-object reconstruction technique. To better capture the complex geometry of dental structures, tetrahedron elements were considered in the model, as in Figure 4, to provide improved conformity to irregular anatomical contours and allow for more accurate representation of stress distribution.

Structural differences between the models are highlighted through the comparison of node and element counts in Figure 7, as a result of utilizing the multi-object reconstruction approach. These differences could potentially impact stability, however, by ensuring adequate mesh density for accurate force transmission across different model components, especially in more complex designs (Models A and B), structural integrity was maintained. Computational efficiency was improved in the simpler, homogeneous structures of endocrowns (Models C and D) as a result of reducing the number of elements and computational demands. In addition, conventional prosthetic designs (Models A and B) included multiple components such as the fibre post, resin core, and crown, leading to a higher number of nodes and elements. In contrast, endocrowns (Models C and D) featured a homogeneous design that eliminated the need for a resin core and fibre post, which reduced the complexity of the mesh and the total number of nodes and elements.

Additional FEA were conducted to verify the stability and suitability of the models for future analysis. Model stability was assessed by evaluating the structural integrity upon loading. This included the absence of significant deformations or irregular stress concentrations. On the other hand, suitability was determined based on mesh quality and sensitivity and load transfer across different model elements and components. Table 5 demonstrates Modified von Mises stress values (MPa) across model components. Monolithic zirconia raises restoration stress in both designs in addition to enamel stress in endocrowns. Switching from crown to endocrown approximately doubles stresses in enamel and dentin for both materials, with enamel exceeding dentin. Doubling the load produced proportional increases across primary readouts with $R \approx 2.00$ (deviation ≤1%-2%), confirming linear elastic scaling. These monotonic, rank-preserving differences are consistent with the model's verified behaviour (≤5% mesh-refinement change; ~2 × scaling at 2 × load) under the stated bonded-interface and boundary-condition assumptions.

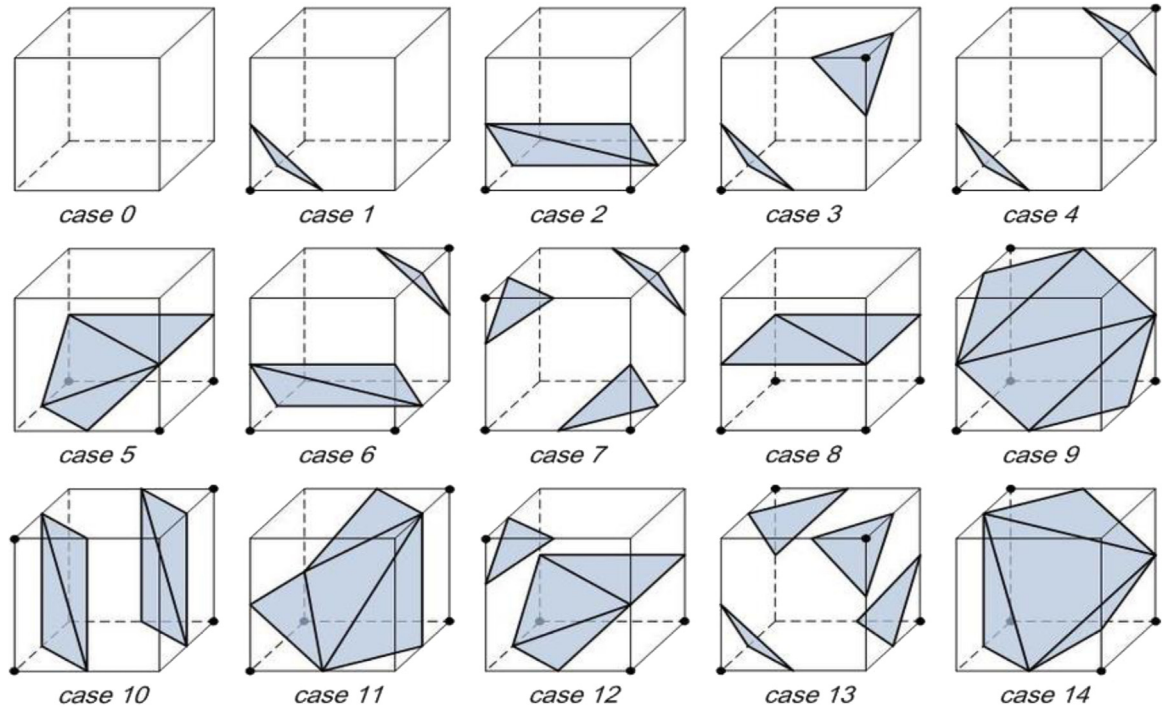

Fig. 3 – Type of surface combinations for the marching cube algorithm, black circles represent vertices inside the surface.[63]

Table 3 – Summary of the individual solid mesh data for the different objects constituting conventional prosthesis (Fibre post, Resin Core, and Crown).

Object	Number of nodes	Number of elements
Crown	3250	2148
Resin core	3112	1885
Fibre post	2998	1817
Resin cement	2219	1345
Gutta percha	2536	1538
Enamel	3620	2195
Dentin	2610	1583
Cementum	3195	1937
PDL (Periodontal ligament)	3260	1975
Alveolar bone	5435	3295
Complete model	33,235	19,718

Table 4 – Summary of the individual solid mesh data for the different objects constituting the endocrown.

Object	Number of nodes	Number of elements
Crown	5785	3385
Resin cement	2219	1345
Gutta percha	2536	1538
Enamel	3620	2195
Dentin	2610	1583
Cementum	3195	1937
PDL (Periodontal ligament)	3260	1975
Alveolar bone	5435	3295
Complete model	28,660	17,253

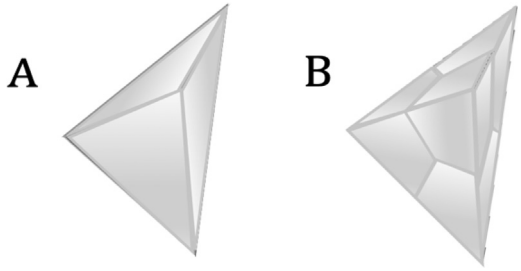

Fig. 4 – (A) Tetrahedral element, (B) Tetrahedral element split into four nodes.

Figure 8 illustrates exploded FE models across components following FE simulations, in which all models demonstrated structural stability and integrity given their ability to withstand occlusal forces. This indicates the suitability of the models for future analyses under different clinical loading conditions.

Figure 9 presents the elastic moduli and Poisson's ratios of different materials and biological structures used in the models. Material properties significantly influenced the outcomes of FEA as given by the pattern of stress distribution and deformation behaviour upon loading. For instance, materials with higher elastic moduli, such as zirconia, significantly reduced structural deformation, which contributed to the observed stability. On the other hand, materials with higher Poisson's ratios enhanced the overall load-bearing capacity of the models through lateral stress distribution. The homogeneous design of the endocrowns resulted in simpler stress distribution patterns, while the more complex structure of conventional prosthetic designs resulted in greater stress distribution and load absorption, especially in the case of Enamel.

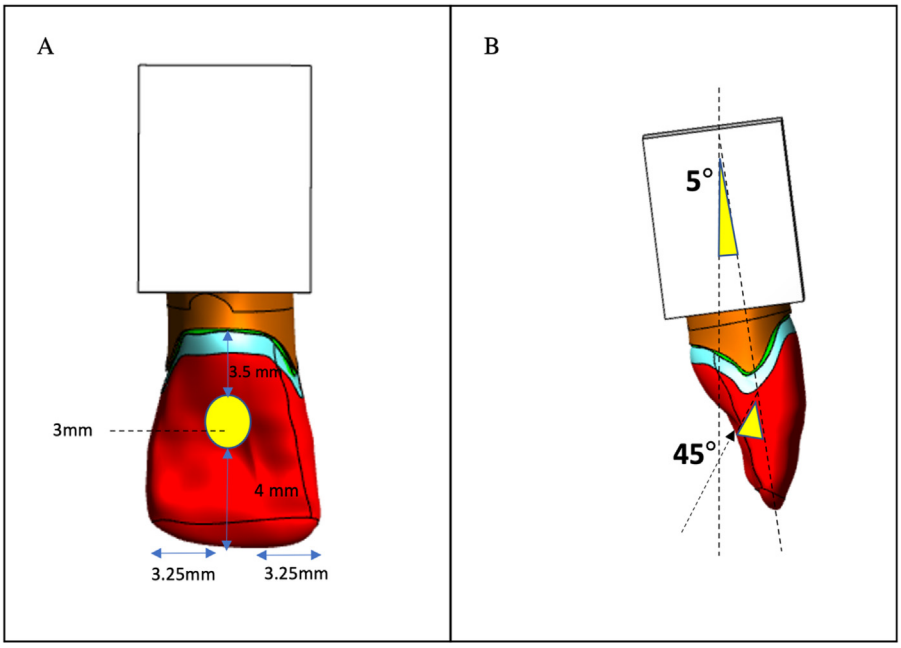

Fig. 5 – (A) A static load of 100 N perpendicularly applied to a circular area with a 3 mm diameter, cantered on the lingual fossa, (B) The model was at a 5° angle procline and the load was oriented at a 45° angle to the long axis of the tooth.

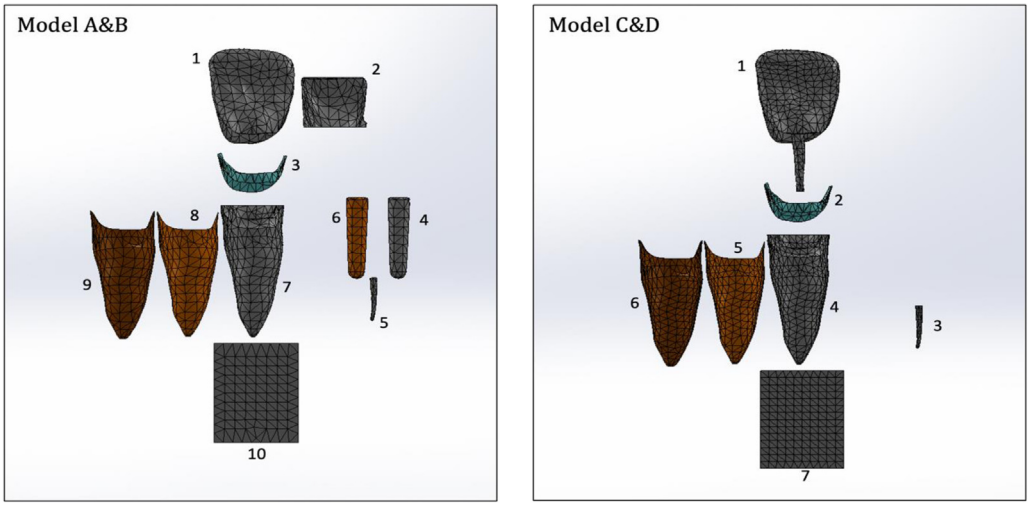

Fig. 6 – Exploded mesh models receiving conventional prosthetic treatment (A and B): Crown 1, Resin core 2, Enamel 3, Fibre post 4, Gutta-percha 5, Resin cement 6, Dentin 7, Cementum 8, PDL 9, Alveolar bone 10. In addition to exploded mesh models receiving endocrowns (C and D): endocrown 1, Enamel 2, Gutta-percha 3, Dentin 4, Cementum 5, PDL 6, Alveolar bone 7.

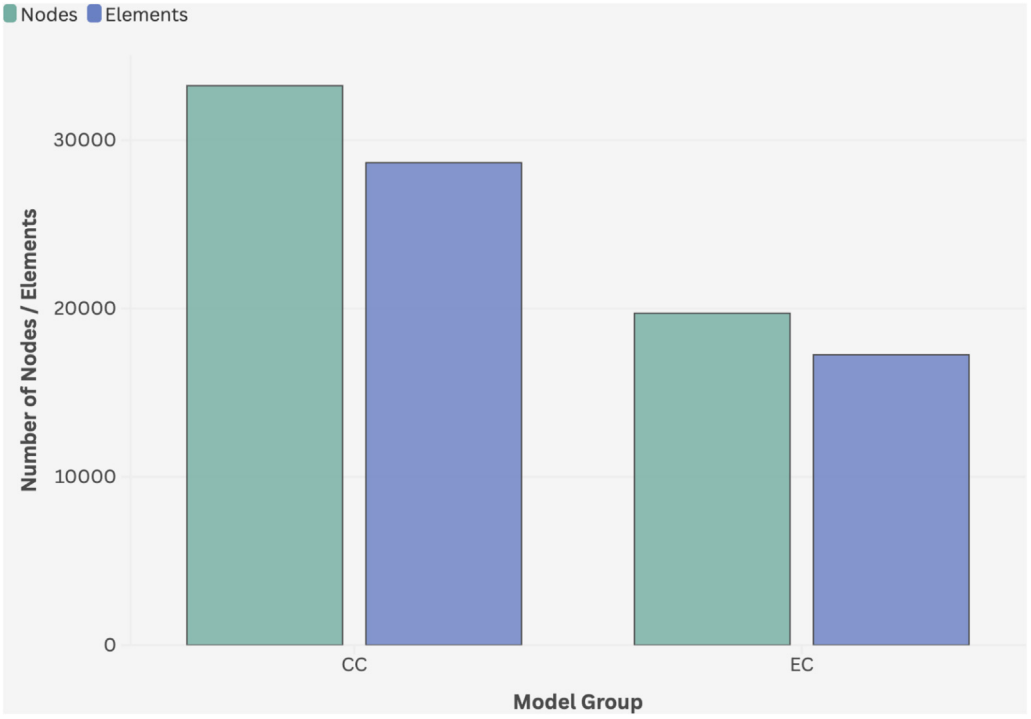

Fig. 7 – Bar chart comparing the total number of nodes and elements between the CC group (Conventional Prosthesis) and the EC group (endocrown).

Table 5 – Modified von Mises stress distribution (MPa) across crown, enamel, and dentin in models A, B, C, and D under 100N loads.

Structure	A	B	C	D
Crown	57.063	84.233	94.261	125.933
Enamel	76.477	80.110	156.106	203.377
Dentin	31.261	31.784	59.354	61.135

Discussion

The complexity of the oral environment necessitates rigorous assessments of new treatment designs and materials. These assessments must consider various factors, including the mechanical and physical properties of dental structures, the magnitude and direction of loads, and the appropriate selection of materials.[3] Additionally, the location of the treated tooth, as well as the patient's general health and oral hygiene, are crucial considerations for clinical success. To ensure that

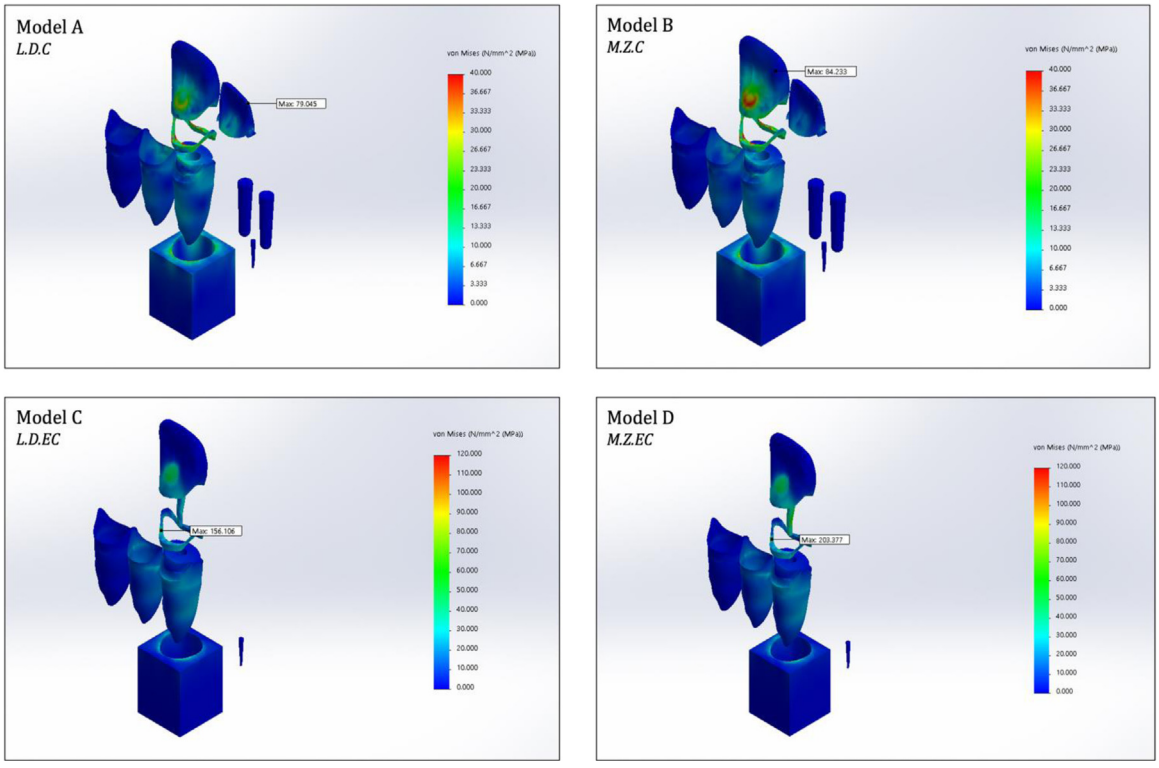

Fig. 8 – Exploded FE models showing various degrees of stress distribution following preliminary FEM simulations. Models received conventional prosthetic lithium disilicate crown (A), monolithic zirconia crown (B), lithium disilicate endocrown (C), monolithic zirconia endocrown (D).

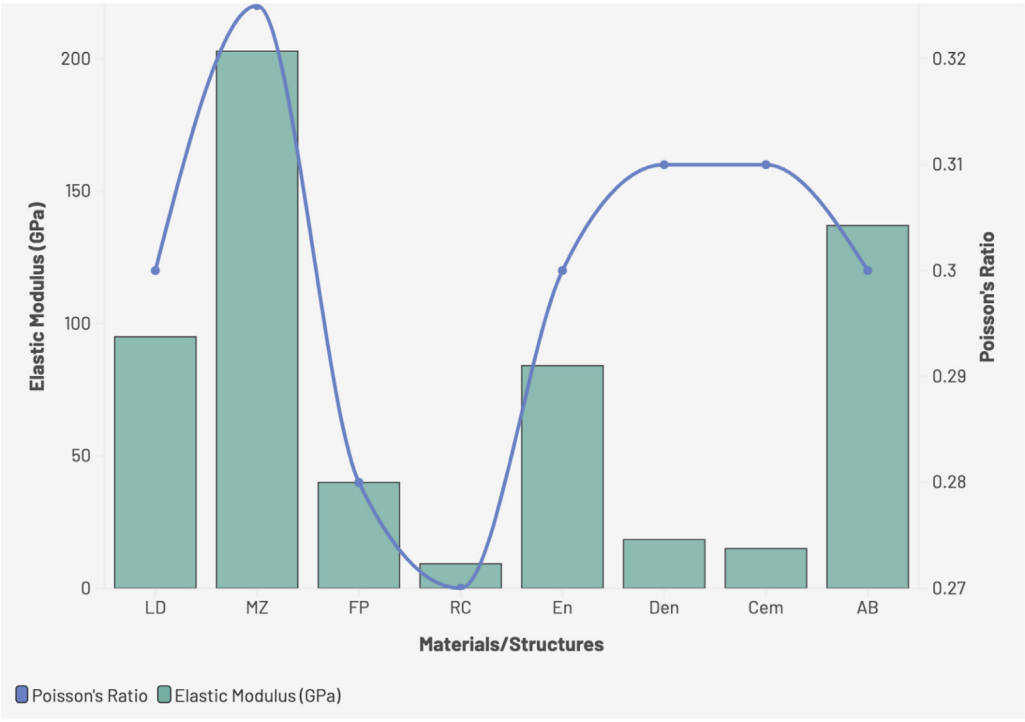

Fig. 9 – Dual-axis chart displaying the Elastic modulus (bar chart) and Poisson's ratio (line graph) for various materials and dental structures used in modelling and restoration.

study results are clinically significant and relevant, scientists strive to closely replicate the physical dimensions and mechanical properties of oral structures, leading to more accurate outcomes.

This study aims to verify the stability and suitability of the proposed methodological framework by building digital dental models using 3D multi-object reconstruction and FEA. Models were constructed with key biological structures integrated using dimensions and properties based on reported literature. These structures included alveolar bone, periodontal ligament, cementum, dentin, enamel, root canal, and apical foramen. Conventional crowns and endocrowns were designed according to established guidelines. This proposed methodology offers a patient-independent, benchmarked-to-published evidence FEM workflow as an alternative to traditional imaging-dependent approaches (CT, CBCT, Intra-oral scanners, Multiple View Image Capture method, 2-dimensional photographs and radiographs, and the bio-CAD method).[8,75,76] According to our results, this technique proved its effectiveness in producing anatomical and structural details with great precision, overcoming challenges of imaging dependent methodologies such as resolution limitations, imaging artifacts, noise, and poor soft tissue contrast.[9,77]

Combining the 3D multi-object reconstruction technique with FEA have produced stable models with structural integrity, showing no significant deformations or irregular stress concentrations upon loading. Indeed, digital 3D reconstruction has been reported to provide precise anatomical data, which aid in the success of many complicated surgical operations, resulting in improved patient outcomes and quality of life.[78] By constructing multi-objects separately and then assembling them to form a complete tooth model, this method allowed for consistent load transmission across elements, resulting in reliable and realistic models, which is beneficial especially in cases where imaging is unavailable or unfeasible.

Differences in node/element counts across designs (Figure 7) capture model complexity and, in turn, computational cost. Simpler assemblies (eg, endocrowns) yield smaller meshes, enabling rapid reruns under consistent geometry and boundary conditions. Standardised FEM's also support parametric sweeps (materials, adhesive/interface specs, cavity geometry), sensitivity checks to assess assumptions before lab work, pre-experiment planning (load, contact areas), benchmarking across sites, and reusable teaching/assessment cases. Over time, a model library becomes a reference set that enables replication, curriculum alignment, and use in resource-limited environments.

This study was carried out with the aim of establishing a foundation for model creation and verification. Material selection, treatment designs, and their response to various loading conditions are beyond the scope of this paper. Future studies will expand on these aspects by assessing the biomechanical behaviour of these models under static and dynamic loads to represent the complex dynamic of the oral environment. These studies will validate the suitability of this methodology in assessing restorative dental treatments.

Reliance on reported material and dimensional parameters in the literature might limit adaptability especially in atypical cases. An additional limitation is the absence of continuous circumferential ferrule was intended for the model; however, a 2 mm ferrule was created on the labial and palatal surfaces which are crucial for the fracture resistance and retention of the crown in anterior endodontically treated maxillary teeth,[60,61] while the mesial and distal surfaces lacked a ferrule. An attempt to overcome this limitation, mesial and distal 2 mm projections or plugs were created to produce a harmonious continuation of the labial and palatal ferrule. Future studies should aim for a full circumferential ferrule to investigate its biomechanical benefits under various loading conditions.

Follow-up studies should include an in-vitro or in-silico cross validation, comparing surface strain and hotspot location under static and dynamic loads to the FE predictions. Add a targeted sensitivity and uncertainty pass eg, moduli ±10%, load angle 45° ± 5°, cement thickness ±50% to identify which inputs materially affect conclusions. Finally, improve reproducibility by packaging the build, mesh, solve into a semiautomated pipeline with auto-generated QA (mesh quality, convergence, linearity) enabling consistent reruns.

Conclusions

Creating stable dental models with great anatomical precision is fundamental for achieving realistic and clinically relevant outcomes. In this study, we presented and verified a digital modelling approach that integrates 3D multi-object reconstruction and FEM to generate dental models with enhanced anatomical accuracy and biomechanical reliability. By constructing models based on evidence-based material properties and dimensions, this approach overcomes limitations associated with traditional imaging techniques, such as resolution constraints, artifacts, and interpatient variability. Accordingly, the proposed standardised model is useful when imaging is not feasible and for educational, research, and low-resource contexts. The FEA confirmed the structural integrity and stability of the generated models under a 100 N static load, demonstrating their potential for use in subsequent biomechanical analysis. Furthermore, the multi-object reconstruction technique facilitated precise control over model components and load transmission, contributing to the realism of the simulations. Although this study acknowledges limitations, including the reliance on literature-reported parameters and the simplification of the ferrule design, it provides a methodological framework for creating dental digital models that closely approximate real-world conditions. This framework can serve as a valuable tool for assessing dental treatments, optimizing restorative designs, and ultimately improving patient outcomes.

Author contributions

Conceptualization: AlKahtani
Methodology: AlKahtani, Allawi, Altassan and AlShalawi
Software: Nassef, Aladhyania and Allawi
Validation: AlKahtani, Nassef and Altassan
Formal analysis: AlKahtani, Allawi and AlShalawi
Investigation: AlKahtani and Aladhyania

Resources: AlKahtani, Nassef and Allawi
Data curation: AlKahtani, Nassef and Allawi
Writing – original draft preparation: AlKahtani and Allawi
Writing – review and editing: AlKahtani, Allawi and Nassef
Visualization: Nassef and Allawi
Supervision: AlKahtani
Project administration: AlKahtani

Availability of data and materials

The datasets used and/or analysed during the current study are available from the corresponding author on reasonable request.

Conflict of interest

None disclosed.

Funding

Authors would like to thank Princess Nourah bint Abdulrahman University Researchers Supporting Project number (PNURSP2025R490), Princess Nourah bint Abdulrahman University, Riyadh, Saudi Arabia.

REFERENCES

1. Gupta M. Digital Diagnosis and Treatment Planning. Cham: Springer International Publishing; 2021. p. 29–63.
2. Samaranayake L, Tuygunov N, Schwendicke F, et al. The transformative role of artificial intelligence in dentistry: a comprehensive overview. Part 1: fundamentals of ai, and its contemporary applications in dentistry. Int Dent J 2025;75 (2):383–96.
3. Tuygunov N, Samaranayake L, Khurshid Z, et al. The transformative role of artificial intelligence in dentistry: a comprehensive overview part 2: the promise and perils, and the international dental federation communique. Int Dent J 2025;75(2):397–404.
4. Sohrabniya F, Hassanzadeh-Samani S, Ourang S A, et al. Exploring a decade of deep learning in dentistry: a comprehensive mapping review. Clin Oral Investig 2025;29(2):1–18.
5. Semerci ZM, Yardımcı S. Empowering modern dentistry: the impact of artificial intelligence on patient care and clinical decision making. Diagnostics 2024;14(12):1260.
6. Alaoffey AS, Asiri MA, Alhazmi TAA, et al. Digital dentistry: transforming diagnosis and treatment planning through CAD/CAM and 3D printing. Egypt J Chem 2024.
7. Pennati F, Aliboni L, Aliverti A. Modeling realistic geometries in human intrathoracic airways. Diagnostics 2024;14(17):1979.
8. Nassef TM. Computer-assisted system to generate a new intelligent rotary dental files IRDF models. Procedia Comput Sci 2015;61:442–7.
9. Sun Y. Prosthesis repair of oral implants based on artificial intelligence finite element analysis. SLAS Technol 2024;29 (6):100226.
10. Lu Jiaxin, Liang Yongqing, Han Huijun, Hua Jiacheng, Jiang Junfeng, Li Xin, Qixing Huang. A survey on computational solutions for reconstructing complete objects by reassembling their fractured parts. Comput Graph Forum 2025:e70081. doi: 10.1111/cgf.70081.
11. Zhang C, Elgharib M, Fox G, Gu M, Theobalt C, Wang W. An implicit parametric morphable dental model. ACM Trans Graph (TOG) 2022;41(6):1–13.
12. Mahmood R, Hamandi SJ, Al-Mahdi AH. Creating a digital 3D model of the dental cast using structure-from-motion photogrammetry technique. Int J Online Biomed Eng (iJOE) 2023;19 (03):4–17.
13. Atif M, Tewari N, Reshikesh M, Chanda A, Mathur VP, Morankar R. Methods and applications of finite element analysis in dental trauma research: a scoping review. Dental Traumatol 2024;40(4):366–88.
14. Shayanfard P, Tan X, Karl M, Wendler F. Finite element combined design and material optimization addressing the wear in removable implant prosthodontics. J Funct Biomater 2024;15(11):344.
15. Serrato-Pedrosa JA, Villanueva-Fierro I, Marquet-Rivera RA, Hernández Vázquez RA, Cruz-Lopez S, Loera-Castañeda V. Non-linear biomechanical evaluation and comparison in the assessment of three different piece dental implant systems for the molar region: a finite element study. J Funct Biomater 2025;16(1):17.
16. Beltrán-Guijarro M, Perez-Pevida E, Chávarri-Prado D, et al. Biomechanical effects of ti-base abutment height on the dental implant system: a finite element analysis. J Funct Biomaterials 2024;15(4):101.
17. Wheeler RC. Dental anatomy, physiology, and occlusion. Philadelphia, PA, USA; 1974.
18. Hu J, Dai N, Bao Y, Gu W, Ma J, Zhang F. Effect of different coping designs on all-ceramic crown stress distribution: a finite element analysis. Dental Mater 2013;29(11):e291–8.
19. Shaikh SY, Shaikh SS. Direct linear measurement of root dentin thickness and dentin volume changes with post space preparation: a cone-beam computed tomography study. Contemp Clin Dent 2018;9(1):77–82.
20. Gupta M, Madhok K, Kulshrestha R, Chain S, Kaur H, Yadav A. Determination of stress distribution on periodontal ligament and alveolar bone by various tooth movements–a 3D fem study. J Oral Biol Craniofac Res 2020;10(4):758–63.
21. Vikram NR, Kumar KS, Nagachandran K, Hashir YM. Apical stress distribution on maxillary central incisor during various orthodontic tooth movements by varying cemental and two different periodontal ligament thicknesses: a fem study. Ind J Dental Res 2012;23(2):213–20.
22. Newman MG, Takei H, Klokkevold PR, Carranza FA. Newman and Carranza's Clinical Periodontology E-Book. Philadelphia, PA, USA: Elsevier Health Sciences; 2018.
23. Gualdi-Russo E, Saguto I, Frisoni P, Neri M, Rinaldo N. Tooth cementum thickness as a method of age estimation in the forensic context. Biology (Basel) 2022;11(5):784.
24. Loukas M, Tubbs RS, Abrahams PH, Carmichael SW, Gest T. Gray's Anatomy Review E-Book. Philadelphia, PA, USA: Elsevier Health Sciences; 2021.
25. Ritter AV. Sturdevant's Art & Science of Operative Dentistry-E-Book. St. Louis, MO, USA: Elsevier Health Sciences; 2017.
26. Benazzi S, Nguyen HN, Kullmer O, Hublin J-J. Unravelling the functional biomechanics of dental features and tooth wear. PLoS One 2013;8(7):e69990.
27. Negreiros WAd, Regis RR, Pontes KMdF, Silva AMd. Silva Junior F.I.d. Effect of restoration technique on stress distribution in extensively destroyed premolars: a finite element analysis study, RGO-Revista Gaúcha de. Odontol Mexico 2017;65:20–4.
28. Heimes D, Schiegnitz E, Kuchen R, Kämmerer PW, Al-Nawas B. Buccal bone thickness in anterior and posterior teeth – a systematic review. Healthcare, 9. BASEL, SWITZERLAND: MDPI; 2021. p. 1663.

29. Fuentes R, Flores T, Navarro P, Salamanca C, Beltrán V, Borie E. Assessment of buccal bone thickness of aesthetic maxillary region: a cone-beam computed tomography study. J Periodontal Implant Sci 2015;45(5):162–8.
30. Januário AL, Duarte WR, Barriviera M, Mesti JC, Araújo MG, Lindhe J. Dimension of the facial bone wall in the anterior maxilla: a cone-beam computed tomography study. Clin Oral Implants Res 2011;22(10):1168–71.
31. Han JY, Jung GU. Labial and lingual/palatal bone thickness of maxillary and mandibular anteriors in human cadavers in koreans. J Periodontal Implant Sci 2011;41(2):60.
32. Do TA, Shen Y-W, Fuh L-J, Huang H-L. Clinical assessment of the palatal alveolar bone thickness and its correlation with the buccolingual angulation of maxillary incisors for immediate implant placement. Clin Implant Dent Relat Res 2019;21(5):1080–6.
33. Cho H-J, Jeon J-Y, Ahn S-J, Lee S-W, Chung J-R, Park C-J, Hwang K-G. The preliminary study for three-dimensional alveolar bone morphologic characteristics for alveolar bone restoration. Maxillofac Plast Reconstr Surg 2019;41:1–7.
34. Vellini-Ferreira F, Cotrim-Ferreira FA, Ribeiro JA, Ferreira-Santos RI. Mapping of proximal enamel thickness in permanent teeth. Braz J Oral Sci 2012;11:481–5.
35. Sandhya V, Arun A, Reddy VP, Mahendra S, Aravind BC. Biomechanical effects of torquing on upper central incisor with thermoplastic aligner: a comparative three-dimensional finite element 22 study with and without auxillaries. J Ind Orthodont Soc 2022;56(1):49–56.
36. Rosenstiel SF, Land MF, Walter R. Contemporary fixed prosthodontics-e-book. Philadelphia, PA, USA: Elsevier Health Sciences; 2022.
37. Alothmani OS, Chandler NP, Friedlander LT. The anatomy of the root apex: a review and clinical considerations in endodontics. Saudi Endodont J 2013;3(1):1–9.
38. Shenoy A, MALA K. Endodontics: Principles and Practice E-book. RELX India Pvt. Ltd.: Elsevier Health Sciences; 2016.
39. Meira JB, Espósito CO, Quitero MF, Poiate IA, Pfeifer CSC, Tanaka CB, Ballester RY. Elastic modulus of posts and the risk of root fracture. Dental Traumatol 2009;25(4):394–8.
40. Tribst JPM, Dos Santos AFC, da Cruz Santos G, da Silva Leite LS, Lozada JC, Silva-Concílio LR, Baroudi K, Amaral M. Effect of cement layer thickness on the immediate and long-term bond strength and residual stress between lithium disilicate glass-ceramic and human dentin. Materials 2021;14(18):5153.
41. Aker Sagen M, Dahl JE, Matinlinna JP, Tibballs JE, Rønold HJ. The influence of the resin-based cement layer on ceramic-dentin bond strength. Eur J Oral Sci 2021;129(4):e12791.
42. de Andrade G-S, Bottino M-A, Valandro L-F, Özcan M, et al. A study on stress distribution to cement layer and root dentin for post and cores made of cad/cam materials with different elasticity modulus in the absence of ferrule. J Clin Exp Dent 2019;11(1):e1.
43. Furuichi T, Takamizawa T, Tsujimoto A, Miyazaki M, Barkmeier WW, Latta MA. Mechanical properties and sliding-impact wear resistance of self-adhesive resin cements. Oper Dent 2016;41(3):E83–92.
44. Chiba A, Hatayama T, Kainose K, et al. The influence of elastic moduli of core materials on shear stress distributions at the adhesive interface in resin built-up teeth. Dent Mater J 2017;36(1):95–102.
45. Li X, Kang T, Zhan D, Xie J, Guo L. Biomechanical behavior of endocrowns vs fiber post-core-crown vs cast post-core-crown for the restoration of maxillary central incisors with 1 mm and 2 mm ferrule height: a 3D static linear finite element analysis. Medicine (Baltimore) 2020;99(43):e22648.
46. Fragkouli M, Tzoutzas I, Eliades G. Bonding of core build-up composites with glass fiber-reinforced posts. Dent J (Basel) 2019;7(4):105.
47. Özkir SE. Effect of restoration material on stress distribution on partial crowns: a 3D finite element analysis. J Dent Sci 2018;13(4):311–7.
48. Shetty PP, Meshramkar R, Patil KN, Nadiger RK. A finite element analysis for a comparative evaluation of stress with two commonly used esthetic posts. Eur J Dent 2013;7(04):419–22.
49. de Carvalho MA, Lazari-Carvalho PC, Cury AA, Magne P. Accelerated fatigue resistance of endodontically treated incisors without ferrule restored with CAD/CAM endocrowns. Int J Esthetic Dentistry 2021;16((4).
50. Li X, Kang T, Zhan D, Xie J, Guo L. Biomechanical behavior of endocrowns vs fiber post-core-crown vs cast post-core-crown for the restoration of maxillary central incisors with 1 mm and 2 mm ferrule height: a 3D static linear finite element analysis. Medicine (Baltimore) 2020;99(43):e22648.
51. Isgrʻo G, Rodi D, Sachs A, Hashimoto M. Modulus of elasticity of two ceramic materials and stress-inducing mechanical deformation following fabrication techniques and adhesive cementation procedures of a dental ceramic. Int J Biomater 2019;2019(1):4325845.
52. Bergoli CD, Meira JBC, Valandro LF, Bottino MA. Survival rate, load to fracture, and finite element analysis of incisors and canines restored with ceramic veneers having varied preparation design. Oper Dent 2014;39(5):530–40.
53. Díaz M, Smirnov A, Gutiérrez-González C, Estrada D, Bartolomé JF. Microstructure and mechanical properties of zirconia (3y-tzp)/zr composites prepared by wet processing and subsequent spark plasma sintering. Ceramics 2020;3(1):53–64.
54. Da Silva NR, Raposo LHA, Versluis A, Fernandes-Neto AJ, Soares CJ. The effect of post, core, crown type, and ferrule presence on the biomechanical behavior of endodontically treated bovine anterior teeth. J Prosthet Dent 2010;104(5):306–17.
55. Juloski J, Radovic I, Goracci C, Vulicevic ZR, Ferrari M. Ferrule effect: a literature review. J Endod 2012;38(1):11–9.
56. Adanir N, Belli S. Evaluation of different post lengths' effect on fracture resistance of a glass fiber post system. Eur J Dent 2008;2(01):23–8.
57. Bitter K, Perdig~ao J, Exner M, Neumann K, Kielbassa A, Sterzen-bach G. Reliability of fiber post bonding to root canal dentin after simulated clinical function in vitro. Oper Dent 2012;37(4):397–405.
58. Shivani S, Vandana K. Assessment of gingival sulcus depth, in primary, mixed and permanent dentition-part-1. Int J Dent Res 2017;5(2):130.
59. Gargiulo AW, Wentz FM, Orban B. Dimensions and relations of the dentogingival junction in humans. J Periodontol (1930) 1961;32(3):261–7.
60. Kaewtip K, Kukiattrakoon B, Sattapan B, Thammasitboon K, White RR. The effect of incomplete crown ferrules on fracture resistance and the failure modes of endodontically treated maxillary incisors restored with cast posts, cores, and crowns. J Orofac Sci 2018;10(1):37–41.
61. Koosha S, Jebelizadeh MS, Mostafavi AS. Effect of ferrule location on fracture resistance of maxillary premolars: an in vitro study. Int J Dent 2023;2023(1):9513804.
62. Al-Wahadni A, Gutteridge D. An in vitro investigation into the effects of retained coronal dentine on the strength of a tooth restored with a cemented post and partial core restoration. Int Endod J 2002;35(11).
63. Nassef T. Computer-assisted tissue engineering for dental applications: Multi-object reconstruction technique. London, UK: LAP Lambert Academic Publishing; 2012.

64. MathWorks. MATLAB, Version R2023b. Natick, Massachusetts: The MathWorks, Inc.; 2023 https://www.mathworks.com/.
65. Wang X, Gao S, Wang M, Duan Z. A marching cube algorithm based on edge growth. Virtual Reality Intell Hardware 2021;3(4):336–49.
66. ANSYS Inc.. ANSYS® Academic Research Mechanical, Release 14.0. Canonsburg, PA, USA: ANSYS Inc; 2013 https://www.ansys.com.
67. J Chen, L Xu, A finite element analysis of the human temporomandibular joint (1994).
68. APerez del Palomar, Doblaŕe M. Anterior displacement of the tmj disk: repositioning of the disk using a mitek system. A 3D finite element study. Journal of Biomedical Engineering 2006;128(5):663–73. doi: 10.1115/1.2246238.
69. Barrett TJ, Savage DJ, Ardeljan M, Knezevic M. An automated procedure for geometry creation and finite element mesh generation: application to explicit grain structure models and machining distortion. Comput Mater Sci 2018;141:269–81.
70. Merema BBJ, Kraeima J, Glas HH, Spijkervet FK, Witjes MJ. Patient-specific finite element models of the human mandible: lack of consensus on current set-ups. Oral Dis 2021;27(1):42–51.
71. Koolstra J, Van Eijden T. Prediction of volumetric strain in the human temporomandibular joint cartilage during jaw movement. J Anat 2006;209(3):369–80.
72. Lee C, Lee P-S. A new strain smoothing method for triangular and tetrahedral finite elements. Comput Methods Appl Mech Eng 2018;341:939–55.
73. Turk AG. The effect of marginal preparation type on an all-ceramic anterior crown: a finite element study. Cumhuriyet Dental J 2017;19(3):214–21.
74. Seymour KG, Cherukara GP, Samarawickrama DY. Stresses within porcelain veneers and the composite lute using different preparation designs. Journal of Prosthodontics 2001;10(1):16–21.
75. Ali FI, Al-dahan ZT. Teeth model reconstruction based on multiple view image capture. IOP Conference Series: Materials Science and Engineering. IOP Publishing; 2020:012009.
76. Silvester CM, Hillson S. A critical assessment of the potential for structure-from-motion photogrammetry to produce high fidelity 3D dental models. Am J Phys Anthropol 2020;173(2):381–92.
77. Venkatesh E, Elluru SV. Cone beam computed tomography: basics and applications in dentistry. J Istanb Univ Fac Dent 2017;51(3 Suppl 1):102–21.
78. Cornejo J, Cornejo-Aguilar JA, Vargas M, et al. Anatomical engineering and 3D printing for surgery and medical devices: international review and future exponential innovations. Biomed Res Int 2022;2022(1):6797745.